Surface defects induced ferromagnetism in mechanically milled nanocrystalline ZnO

Srabantika Ghose, A. Sarkar, S. Chattopadhyay, M. Chakrabarti, D. Das, T. Rakshit, S. K. Ray, and D. Jana

Citation: Journal of Applied Physics **114**, 073516 (2013); doi: 10.1063/1.4818802
View online: http://dx.doi.org/10.1063/1.4818802
View Table of Contents: http://scitation.aip.org/content/aip/journal/jap/114/7?ver=pdfcov
Published by the AIP Publishing

Surface defects induced ferromagnetism in mechanically milled nanocrystalline ZnO

Srabantika Ghose,[1] A. Sarkar,[2] S. Chattopadhyay,[3] M. Chakrabarti,[1] D. Das,[4] T. Rakshit,[5] S. K. Ray,[5] and D. Jana[1,a)]
[1]*Department of Physics, University of Calcutta, 92 A. P. C. Road, Kolkata 700009, India*
[2]*Department of Physics, Bangabasi Morning College, 19 R. C. Sarani, Kolkata 700009, India*
[3]*Department of Basic Science and Humanities, Calcutta Institute of Engineering and Management, 24/1A Chandi Ghosh Road, Kolkata 700040, India*
[4]*UGC-DAE Consortium for Scientific Research, III/LB-8, Salt Lake, Kolkata 700098, India*
[5]*Department of Physics and Meteorology, Indian Institute of Technology, Kharagpur 721302, India*

(Received 11 April 2013; accepted 2 August 2013; published online 21 August 2013)

Bulk ZnO is a diamagnetic material but ferromagnetism (FM) has been observed by several groups in its nanostructures. In order to elucidate the room temperature (RT) FM of ZnO nanostructures, magnetic property of mechanically milled and subsequently annealed nano-ZnO powder has been investigated. Sample that has been milled and then annealed at 200 °C in ambient condition shows highest value of saturation magnetization (M_s), whereas lowest value of M_s has been noticed for the sample pre-annealed at 500 °C before milling. The variation of M_s with annealing temperatures closely resembles with the variation of average positron lifetime (τ_{av}) and S-parameter reported earlier for these nano-systems. It has also been found that M_s decreases systematically for increasing average grain size of the ZnO nanoparticles. Room temperature photoluminescence of the as-milled sample shows broad defect related emission centered ~2.23 eV. Enhancement of such emission has been observed due to 200 °C annealing. Results altogether indicate that ferromagnetism in ZnO depends critically on the nature of disorder (open volume defects as well as defect clusters) at the grain surface region. In this connection, the possible role of zinc vacancy defects has also been emphasized. © *2013 AIP Publishing LLC*. [http://dx.doi.org/10.1063/1.4818802]

I. INTRODUCTION

In recent years, dilute magnetic semiconductors (DMSs)[1–8] have attracted researchers because of their favorable magnetic, magneto-optic, and magneto-electric properties. ZnO based DMS systems bear wide band gap (3.37 eV) and large exciton binding energy (~60 meV), which is suitable for application above room temperature (RT) also. A part of the research has been concentrated on transition metal (TM) doping like Fe, Co, Mn, etc., in ZnO. It has been claimed[9] by Garcia *et al*. that double exchange interaction between Mn^{2+} and Mn^{3+} ions in Zn(Mn)O is associated with room temperature ferromagnetism (RTFM). On the other hand, Kundaliya *et al*. have argued[10] that oxygen vacancy rich $Mn_{2-x}Zn_xO_3$ phase at the grain surface contributes to observed ferromagnetism in Mn doped ZnO. For the Co-doped ZnO, Sato and Yoshida have also predicted[11] that ferromagnetism (FM) is a result of double exchange interaction between the Co ions. Jalbout *et al*. have suggested[12] that Ruderman-Kittel-Kasuya-Yosida (RKKY) interaction is responsible for the RTFM in doped ZnO system. Interestingly, X-ray magnetic circular dichroism measurements on Co doped ZnO system have revealed that observed FM is not due to doped TM ions including Co clusters or some secondary phase.[13] So, search for RTFM in undoped ZnO and other metal oxide semiconductors such as TiO_2, In_2O_3, HfO_2, etc., has also been started.[14–18] However, even after so many experimental and theoretical efforts, the correct mechanism of ferromagnetic ordering in such materials, which are diamagnetic in their respective bulk form, is still a topic of debate.

Up to now, it has been understood that FM state in ZnO based materials is stabilized by some native defects or their complexes. So the focus is on ZnO nanostructures, which are defect rich, for the last few years.[15,18–27] There are reports which favor zinc vacancies (V_{Zn}) as a source of FM in ZnO.[20,24,27,28] On the other hand, oxygen vacancy (V_O) or zinc interstitial (I_{Zn}) mediated FM in ZnO has also been claimed by several groups.[15,22,29,30] It has already been argued that not any specific type of defects rather extended defects, defect clusters, and/or non-stoichiometric porous regions particularly at the grain boundaries (GB) are actually the source of FM in ZnO based nano-systems.[18,23] In case of capped ZnO nanoparticles, the interfacial band structure between ZnO and the capping molecule can give rise to FM.[31] It has been claimed that sufficiently high internal electric field due to truncated ZnO lattice along {001} direction (most preferred direction of growth of ZnO crystal) may lead to room temperature FM.[32] In this report, we provide further insight to such debates and discussions. In this carefully planned experiment, it has been noted that open volume defects, particularly V_{Zn} residing at the grain surfaces are the major source of FM in granular ZnO. An increase or decrease of M_s, however, depends critically on the defect structure of grain boundary regions.

a)Author to whom correspondence should be addressed. Electronic mail: djphy@caluniv.ac.in. Tel.: + 91-33-2350 8386 ext. 413. Fax: + 91-33-2351-9755.

Very recently, Phan *et al.*[19] have indicated the key role played by V_{Zn} in observing FM order in ZnO nanoparticles prepared by mechanical milling. However, V_{Zn} mediated FM in undoped ZnO should not be taken as universal. There indeed exist at least two different regimes of carrier concentration for inducing FM in ZnO based systems.[19,33,34] The role of V_{Zn} is particularly critical for insulating ZnO systems with very low concentration of donor defects.[35] To note, all the samples in the present work bear sheet resistances above 200 MΩ/cm^2.

II. EXPERIMENTAL

High purity ZnO (99.99%, Sigma-Aldrich, Germany, impurity level <200 ppm trace metal basis) powder has been ball-milled in an agate container with agate balls (ball to mass ratio 5:1) for 17 h in a Fritsch Pulverisette 6 planetary ball mill grinder. After every 30 min of milling, the milling system is given rest for dissipation of the heat generated and to avoid any unexpected impurity. The ground material has been pressed into pellets and then subsequently annealed at different temperatures (200, 300, 400, 500, 600, and 700 °C) in air for 4 h. A separate sample has been prepared, which is annealed at 500 °C in air and then milled. We will refer this sample as annealed + milled sample.

X-ray diffraction (XRD) patterns of the samples have been recorded in a TTRAX III Rigaku X-ray diffractometer using Cu K_α (1.542 Å) radiation. The average grain sizes of all the samples have been estimated by standard procedure using Scherer's formula[36] with most intense (101) XRD peak of all the samples. The magnetic measurements of all samples have been performed at RT using a superconducting quantum interferometer device (SQUID) magnetometer (MPMS XL 7, Quantum Design, USA). Each measurement is carried with a small amount of sample (~100 ± 20 mg) taken in a plastic straw. Before magnetic measurement, M-H data are recorded for an empty sample holder and no error signal as investigated by Garcia *et al.*[37] has been observed. With the help of non linear fitting, diamagnetic contribution arising from the straw has been subtracted from the measured magnetization (M) versus magnetic field (H) curve to estimate different magnetic parameters.

Photoluminescence (PL) measurements at RT have been carried out with He-Cd laser as an excitation source, operating at 325 nm with an output power of 45 mW and a TRIAX 320 monochromator fitted with a cooled Hamamatsu R928 photomultiplier detector. To detect the defect related PL peaks below 2 eV, if any, a filter at 380 nm has been used.

III. RESULT AND DISCUSSION

Figure 1 represents M vs. H curve for the as-milled sample before annealing. The curve (red line) shows that there is a ferromagnetic signal superimposed on a strong diamagnetic component. After subtraction of the diamagnetic background, the ferromagnetic hysteresis curve is visible in the same figure. The value of saturation magnetization (M_s) for the milled ZnO sample is consistent with other reports on nano-ZnO systems.[34] Similar M-H curves obtained for all the annealed samples have been depicted in Figure 2. The inset of Figure 2 shows M-H curve of the as-supplied sample. It is evident from the inset in Figure 2 that the as-supplied powder is diamagnetic in conformity with the bulk nature of ZnO. From Figure 2, it is clearly seen that the sample which is milled and subsequently annealed at 200 °C has the highest value of M_s (0.0037 ± 0.00005 emu/gm). For annealing above 200 °C, M_s monotonically decreases with increasing annealing temperature. It is interesting to note that M_s is reduced by one order of magnitude (compared to the sample with highest M_s) for annealing at 700 °C.

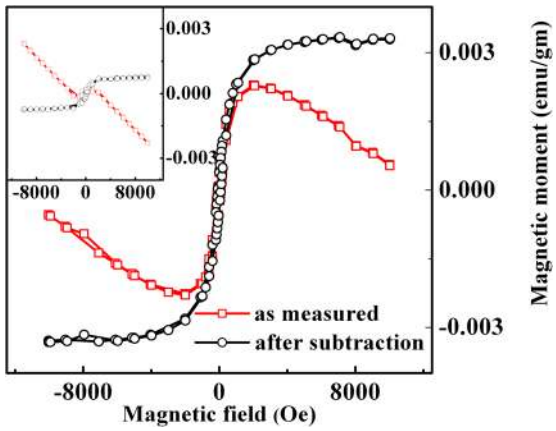

FIG. 1. M-H curve for the as-milled sample at room temperature. The same curve for the sample annealed and then milled is shown as an inset.

It is apparent that annealing above 500 °C seems to be very critical for magnetism in ZnO based systems. In Mn doped ZnO, low sintering temperature (≤500 °C) is preferred to achieve the best ferromagnetic properties.[38] Similar observation exists for ZnO nanoparticles also.[15,29] In fact, Mal *et al.* have observed that M_s is reduced as the duration of annealing at 500 °C increases.[34] In our study, however, a separate batch of sample has been prepared with annealing at 500 °C prior to milling. Conditions of milling have been maintained same as stated in Sec. II. The average grain size of this sample comes out to be 33 nm. However, it is evident from Figure 1 (inset) that M_s for this particular sample is very low (0.0008 emu/gm), lowest among all the measured samples. Possible reasons of such experimental outcome have been discussed later.

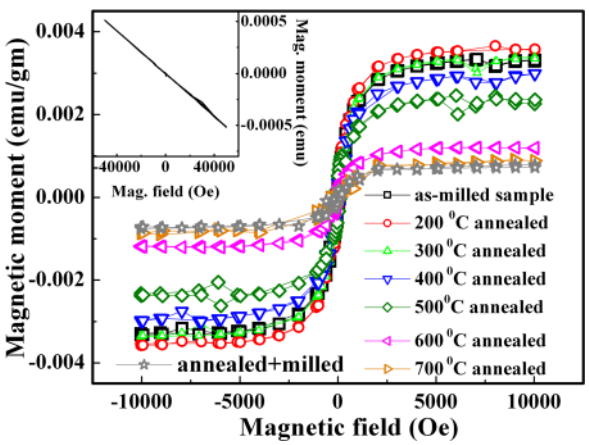

FIG. 2. Similar M-H curves for differently annealed ZnO nanoparticles.

To explore the connection between structural changes and magnetization, we perform XRD of all samples and the resultant patterns have been shown in Figure 3. The variation of average grain size (actually grain diameter, D) with annealing temperature has been indicated as an inset. It is noticed from Figure 3 that the average grain size of ZnO nanocrystals decreases from 80 nm (as-supplied material) to 32 nm due to mechanical milling. Besides, annealing of the as-milled sample at 200 °C causes further reduction of grain size to 30 nm. Although errors in estimated grain sizes are ±2 nm, however, such observation is reproducible.[39,40] This particular feature has been observed in ZnO nanocrystals[41] and thin films[42] also. Interestingly, M_s for the sample annealed at 200 °C is highest. It clearly points out that FM in ZnO nano systems is intrinsic and defect mediated. Annealing at higher temperatures (300–700 °C) causes a monotonic increase of grain size (D) of the samples. If we plot M_s vs. $1/D$, the variation is more or less linear (Figure 4). The parameter $1/D$ can be taken as proportional to the grain surface to volume ratio. In fact, this linear variation of M_s with $1/D$ indicates that FM in ZnO is indeed a grain surface related phenomenon. Li *et al.* have reported[25] proportionality of M_s with $1/D^5$ for ZnO films with $D < 76$ nm. It is not possible to distinguish between two different nature of variations, $1/D^5$ or $1/D$, from our data set. However, the consistency of the results found here with earlier reports should be mentioned. Figure 4 reveals that M_s goes down to zero for $D = 58 \pm 10$ nm. That means for ZnO samples with grain sizes larger than 68 nm, FM is not expected. If we take the specific grain surface area (S_{GB}) as $1.65/D$ (Ref. 18), then the lower limit of S_{GB} for which $M_s \neq 0$ is $(3 \pm 1) \times 10^7$ m^2/m^3. Straumal *et al.* have also found[18] the critical S_{GB} as $(5 \pm 3) \times 10^7$ m^2/m^3 below which no net magnetization has been observed for undoped ZnO. If reduced density of such porous samples is taken into account, then for same D, effective S_{GB} will be higher providing further agreement of our estimation and that by Straumal *et al.*

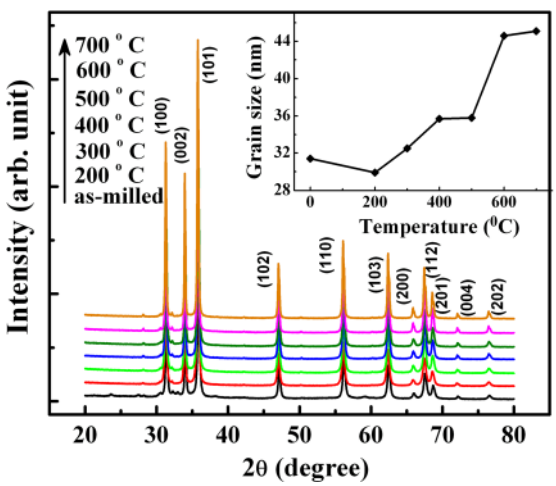

FIG. 3. XRD patterns for the mechanically milled and subsequently annealed ZnO samples. The annealing temperatures have been mentioned in the graph. The variation of grain size with annealing temperature is shown in the inset.

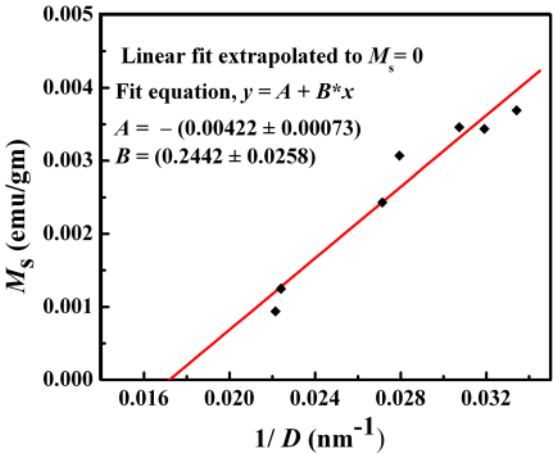

FIG. 4. Variation of saturation magnetization with inverse of average grain size for ZnO samples.

Figure 5 illustrates the variation of M_s and coercivity (H_c) with annealing temperature. Two different regions named as region-I and region-II have been indicated in Figure 5. Region-I is below 500 °C where variations of M_s and H_c with annealing temperature have opposite nature. This is typical for a soft ferromagnet. In fact, opposite variations of M_s and H_c have been observed earlier in nanocrystalline Mn-doped ZnO.[28] However, above 500 °C (region-II), both the parameters decrease with increasing annealing temperature. For the sample annealed at 200 °C, there is a reduction of both H_c and D. However, between 400 and 500 °C annealing there is a sharp rise in the value of H_c although there is no significant change in value of D (Figs. 5 and 3). Highest value of H_c (≈135 ± 10 Oe) has been observed for the sample annealed at 500 °C corresponding to D ≈ 36 nm (inset of Fig. 3). For annealing above 500 °C, there is a reduction of H_c with increment of D. For annealed + milled sample, D ≈ 33 nm. However, it is interesting to note that H_c of this sample ≈105 ± 10 Oe higher in compared to the milled and successively annealed sample with D ≈ 33 nm (for 300 °C annealing). This indicates that H_c is not related to the grain size of the sample as occurred for ordinary ferromagnetic materials. From these observations, one may

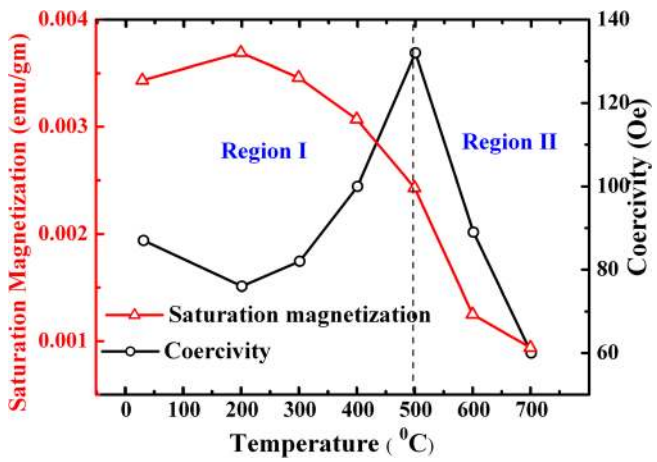

FIG. 5. Variation of saturation magnetization and coercivity with annealing temperature.

conclude that FM of these undoped nano-ZnO samples is related to not only the grain surface area but also to intrinsic defects residing at GB.

The variation of M_s with annealing temperature closely resembles the variation of positron annihilation spectroscopic (PAS) parameters with annealing temperature in nanocrystalline or polycrystalline ZnO (Refs. 39 and 43). To mention, positron spectroscopy probes open volume vacancy defects in solid materials. In nanocrystalline ZnO, PAS parameters are particularly sensitive to the zinc vacancy related changes at the grain surfaces.[28,43] The detailed discussion on *S*-parameter or average positron lifetime can be found in Ref. 40. Our earlier data on this aspect have been shown in Figure 6. It is clear that after initial annealing at 200 °C, S-parameter or average positron lifetime increases in granular ZnO material. It reflects the increment of open volume defects at the grain boundary regions. Reduction of M_s as well as average positron lifetime with annealing above 400 °C has also been reported[27] by Wang *et al*. In this context, present data are in qualitative agreement with that by Wang *et al*.

Possible reason for lowering grain size or the increase of PAS parameters for annealing at 200 °C should be discussed here because it may be related with the enhancement of M_s for that particular sample. Such granular ZnO samples (as-supplied) are mostly prepared by chemical routes, hence presence of −OH ligands either at grain surface or at the bulk[44] is possible. At the same time, some carbon related compound may also be present.[45] Initial stage of annealing (~200 °C) removes such compounds in the form of H_2O or CO_2 along with adsorbed species at the grain surfaces. As a result, more coarsening of grain surface regions takes place. Moreover, the supply of thermal energy promotes defect migration in the bulk and coalescence of open volume defects in the form of clusters. As similarly charged V_{Zn} or V_O defects cannot grow much, most probable defect clusters are $V_{Zn} - V_O$ type. Additional driving force of this coalescence is that the nearest neighbor $V_{Zn} - V_O$ defect is energetically favorable compared to when they are apart.[46] Thus, as a result all such defects will move towards grain surfaces, which are already defect rich and act as universal sink of defects. Theoretical study also predicts that vacancy defects are more stable at the grain surface regions.[20] So, foam-like defective structure of the grain boundary is enhanced due to 200 °C annealing. It appears that some critical concentration of V_{Zn} defects and the surrounding defective network are the key factors in tuning FM in ZnO. In fact, a recent theoretical work has predicted that nearest neighbor $V_{Zn} - V_O$ pair defects as well as V_{Zn} (both in negative charge state) can drive diamagnetic ZnO to ferromagnetic one.[47] Please note that isolated V_{Zn} or V_O defects in the bulk may not generate FM in ZnO.[20,32] Earlier, PAS (experimental[40] or theoretical[48]) and optical absorption spectroscopy[49] have indicated the presence of significant amount of large defect clusters containing V_{Zn} and V_O in granular ZnO. The present study thus confirms the contention and correlates the increase of net ferromagnetic moment of the 200 °C annealed sample with the increase of V_{Zn} related disorder. On annealing above 200 °C, the combination of defect species that generate FM is disturbed. This can be due to two reasons. First-principles theoretical calculation has shown[50] that V_{Zn} defects start to recover just above 250 °C. Experimental results exist in favor of this idea.[39,50] So, reduction of M_s for annealing at 300 °C is possible due to partial recovery of V_{Zn} defects. Due to annealing of ZnO in air at and above 200 °C, generation of oxygen vacancies predominates than their recovery.[51] V_O is a donor type defect in ZnO (Ref. 50). Although deep, such defects or their complexes contribute to conduction band electrons which above certain concentration cause more n-type character in ZnO and impede ferromagnetic interaction.[47] In the present nano-ZnO system, the appearance of isolated V_Os can cause further lowering of M_s. This is why the sample is pre-annealed (at 500 °C) and then milled; chemical balance of defects at GB is different and detected FM is weakest of all.

The room temperature PL spectra of the selected samples have been shown in Figure 7. The filter used is at 380 nm (3.26 eV) and that is why the near band edge PL emission (3.20–3.30 eV) intensity is less reliable. The as-

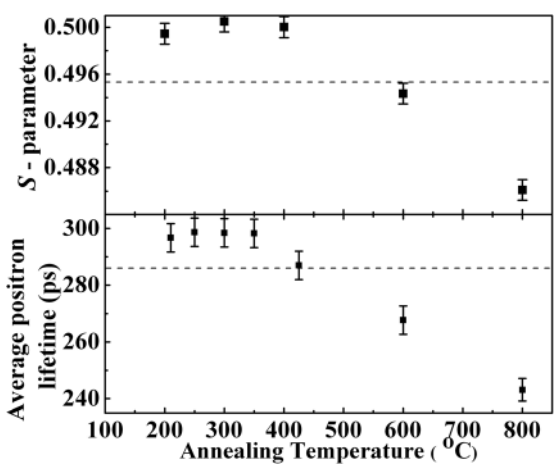

FIG. 6. Variation of average positron lifetime and *S*-parameter with annealing temperature for a different batch of nano-ZnO samples (data taken from Refs. 20 and 24). The dashed lines represent respective values of their unannealed counterparts.

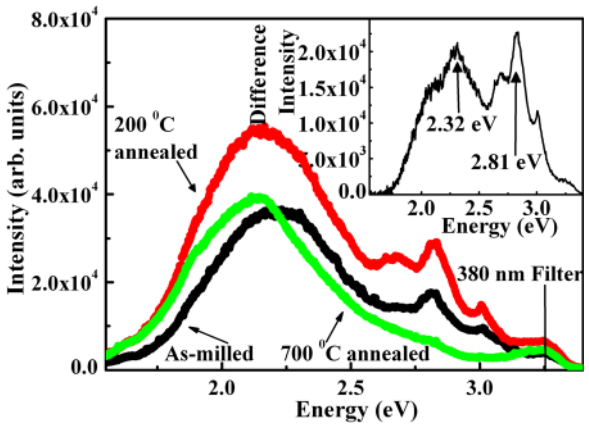

FIG. 7. Room temperature photoluminescence for selected samples. The difference of emission intensity (PL intensity of 200 °C annealed sample minus the same for 700 °C annealed sample) with photon energy is shown in the inset.

milled sample shows broad defect level emission (DLE) around 2.23 eV. This emission can be a mixture of two emissions at 2.14 eV (580 nm) and 2.36 eV (525 nm), mostly found in ZnO nanostructures and thought to originate from doubly and singly ionized oxygen vacancies, respectively, in ZnO. Furthermore, the intensity of the 2.36 eV PL emission is correlated[52,53] with higher value of M_s in ZnO nanowires. In the present work, a redshift of 0.7 eV and increased intensity of the broad DLE peak (~2.23 eV) take place after annealing at 200 °C. This can be due to increase of 2.14 eV emission which, at least to the best of our knowledge, is not related to FM in ZnO. Migration of V_{Zn} defects at the grain boundary due to annealing at 200 °C can enhance the supply of holes in this depletion region. Singly ionized oxygen vacancies capture these holes in the depletion region, thereby changing to doubly ionized vacancies and giving rise to 2.14 eV emission.[52] Reduction of 2.36 eV emission, if it is related to oxygen vacancies, is not expected due to annealing at elevated temperature (700 °C). So, we think that origin of DLE in the present as-milled ZnO is not directly related to oxygen vacancies. In the higher energy side of the spectrum, it can be noticed that PL emission in the range of 2.62–3.10 eV is lowest for the 700 °C annealed sample. The difference of PL intensity (at same energy) between 200 and 700 °C annealed samples has been shown as an inset in Figure 7. Two broad but prominent peaks, ~2.32 and 2.81 eV, can be clearly identified in the difference spectrum. The increased weight of the 2.81 eV emission for 200 °C annealed sample can originate from enhanced grain boundary interface traps and other related defects in the vicinity.[54] Broad DLE peak ~2.8 eV in ZnO nanocrystalline film[55] or powder[49,56] can be understood as a signature of high grain surface area. Keeping track with all the observations mentioned above, we here assign 2.23 eV emission in the as-milled ZnO to zinc vacancies at the grain boundaries. DLE peaks ~2.3 eV have been found earlier in ZnO nanowires[57] and recently in ZnO powder.[58] The 2.3 eV emission at 80 K in ZnO powder has been assigned to V_{Zn} defects.[58] High temperature (700 °C) annealing promotes grain growth and grain boundary related emissions occur with reduced weight as is observed here. So, results altogether indicate the crucial role of grain boundary open volumes, particularly, V_{Zn} type defect clusters in mediating ferromagnetic ordering in undoped ZnO nanoparticles.

IV. CONCLUSION

ZnO powder has been mechanically milled and subsequently annealed at different temperatures in between 200 and 700 °C in air. The as-milled sample with average grain size ~32 nm becomes ferromagnetic at room temperature. In spite of little reduction of average grain size at 200 °C annealing, the average grain size increases with increase of annealing temperature. The highest saturation magnetization has been observed for the sample annealed at 200 °C. The saturation magnetization has been found to depend linearly with the inverse of grain size. However, the sample annealed at 500 °C prior to milling shows very weak ferromagnetism, although grain size of this sample is ~33 nm. Therefore, ferromagnetism in ZnO depends critically on nature of defect clusters at the grain surface region. Combining results of the present study with earlier reported data on positron annihilation spectroscopic investigation in nano-ZnO, the most probable defect species that mediate ferromagnetism in ZnO can be identified as zinc vacancies residing at grain surface regions. Results of room temperature photoluminescence investigation support this possibility.

ACKNOWLEDGMENTS

This work was financially supported by DST-FIST and DST-PURSE, Government of India. We acknowledge Professor R. Ranganathan, Saha Institute of Nuclear Physics (SINP), Kolkata for XRD measurements. Author S.G. gratefully acknowledges University Grant Commission (UGC), Government of India for providing her RFSMS fellowship. We thank the anonymous reviewers for their valuable comments and suggestions to improve the quality of the paper. One of the authors, M.C., also gratefully acknowledges UGC, New Delhi for providing financial assistance through D. S. Kothari post doctoral fellowship.

[1]S. Kolesnik, B. Dabrowski, and J. Mais, J. Appl. Phys. **95**, 2582 (2004).
[2]T. Zhu, W. S. Zhan, W. G. Wang, and J. Q. Xiao, Appl. Phys. Lett. **89**, 022508 (2006).
[3]S. W. Yoon, S. B. Cho, S. C. We, S. Yoon, B. J. Suh, H. K. Song, and Y. J. Shin, J. Appl. Phys. **93**, 7879 (2003).
[4]S.-J. Han, T.-H. Jang, Y. B. Kim, B.-G. Park, J.-H. Park, and Y. H. Jeong, Appl. Phys. Lett. **83**, 920 (2003).
[5]K. R. Kittilstved, D. A. Schwartz, A. C. Tuan, S. M. Heald, S. A. Chambers, and D. R. Gamelin, Phys. Rev. Lett. **97**, 037203 (2006).
[6]K. Ueda, H. Tabata, and T. Kawai, Appl. Phys. Lett.**79**, 988 (2001).
[7]K. R. Kittilstved and D. R. Gamelin, J. Am. Chem. Soc. **127**, 5292 (2005).
[8]Z. X. Cheng, X. L. Wang, S. X. Dou, K. Ozawa, H. Kimura, and P. Munroe, J. Phys. D: Appl. Phys. **40**, 6518 (2007).
[9]M. A. Garcıa, M. L. R. Gonzalez, A. Quesada, J. L. C. Kramer, J. F. Fernandez, S. J. Khatib, A. Wennberg, A. C. Caballero, M. S. M. Gonzalez, M. Villegas, F. Briones, J. M. G. Calbet, and A. Hernando, Phys. Rev. Lett. **94**, 217206 (2005).
[10]D. C. Kundaliya, S. B. Ogale, S. E. Lofland, S. Dhar, C. J. Metting, S. R. Shinde, Z. Ma, B. Varughese, K. V. Ramanujachary, L. S. Riba, and T. Venkatesan, Nature Mater. **3**, 709 (2004).
[11]K. Sato and H. K. Yoshida, Physica E **10**, 251 (2001).
[12]A. F. Jalbout, H. Chen, and S. L. Whittenburg, Appl. Phys. Lett. **81**, 2217 (2002).
[13]M. Gacic, G. Jakob, C. Herbort, H. Adrian, T. Tietze, S. Brück, and E. Goering, Phys. Rev. B **75**, 205206 (2007).
[14]M. Venkatesan, C. B. Fitzgerald, and J. M. D. Coey, Nature (London) **430**, 630 (2004).
[15]A. Sundaresan, R. Bhargavi, N. Rangarajan, U. Siddesh, and C. N. R. Rao, Phys. Rev. B **74**, 161306 (R) (2006).
[16]N. H. Hong, J. Sakai, N. Poirot, and V. Brize, Phys. Rev. B **73**, 132404 (2006).
[17]J. M. D. Coey, Solid State Sci. **7**, 660 (2005).
[18]B. B. Straumal, A. A. Mazilkin, S. G. Protasova, A. A. Myatiev, P. B. Straumal, G. Schütz, P. A. van Aken, E. Goering, and B. Baretzky, Phys. Rev. B **79**, 205206 (2009).
[19]T.-L. Phan, Y. D. Zhang, D. S. Yang, N. X. Nghia, T. D. Thanh, and S. C. Yu, Appl. Phys. Lett. **102**, 072408 (2013).
[20]Q. Wang, Q. Sun, G. Chen, Y. Kawazoe, and P. Jena, Phys. Rev. B **77**, 205411 (2008).
[21]D. Sanyal, M. Chakrabarty, T. Kundu Roy, and A. Chakrabarty, Phys. Lett. A **371**, 482 (2007).
[22]B. Panigrahy, M. Aslam, and D. Bahadur, Appl. Phys. Lett. **98**, 183109 (2011).

[23]R. Podila, W. Queen, A. Nath, J. T. Arantes, A. L. Schoenhalz, A. Fazzio, G. M. Dalpian, J. He, S. J. Hwu, M. J. Skove, and A. M. Rao, Nano. Lett. **10**, 1383 (2010); X. G. Zhao and Z. Tang, J. Appl. Phys. **111**, 084321 (2012).
[24]M. Khalid, M. Ziese, A. Setzer, P. Esquinazi, M. Lorentz, H. Hochmuth, M. Grundmann, D. Spemann, T. Butz, G. Brauer, W. Anwand, G. Fischer, W. A. Adeagbo, W. Hergert, and A. Ernst, Phys. Rev. B **80**, 035331 (2009).
[25]L. Y. Li, Y. H. Cheng, X. G. Luo, H. Liu, G. H. Wen, R. K. Zheng, and S. P. Ringer, Nanotechnology **21**, 145705 (2010).
[26]Q. J. Wang, J. B. Wang, X. L. Zhong, Q. H. Tan, Z. Hu, and Y. C. Zhou, Appl. Phys. Lett. **100**, 132407 (2012).
[27]D. Wang, Z. Q. Chen, D. D. Wang, N. Qi, J. Gong, C. Y. Cao, and Z. Tang, J. Appl. Phys. **107**, 023524 (2010).
[28]S. Chattopadhyay, S. K. Neogi, A. Sarkar, M. D. Mukadam, S. M. Yusuf, A. Banerjee, and S. Bandyopadhyay, J. Magn. Magn. Mater. **323**, 363 (2011).
[29]D. Gao, Z. Zhang, J. Fu, Y. Xu, J. Qi, and D. Xue, J. Appl. Phys. **105**, 113928 (2009).
[30]X. Zhang, Y. H. Cheng, L. Y. Li, H. Lin, X. Zuo, G. H. Wen, L. Li, R. K. Zheng, and S. P. Ringer, Phys. Rev. B **80**, 174427 (2009).
[31]J. Chaboy, R. Boada, C. Piquer, M. A. Laguna-Marco, M. Garcia-Hernandez, N. Carmona, J. Llopis, M. L. Ruíz-González, J. González-Calbet, J. F. Fernandez, and M. A. Garcia, Phys. Rev. B **82**, 064411 (2010).
[32]J. Hong, J. Choi, S. S. Jang, J. Gu, Y. Chang, G. Wortman, R. L. Snyder, and Z. L. Wang, Nano Lett. **12**, 576 (2012).
[33]A. J. Behan, A. Mokhtari, H. J. Blythe, D. Score, X.-H. Xu, J. R. Neal, A. M. Fox, and G. A. Gehring, Phys. Rev. Lett. **100**, 047206 (2008).
[34]S. Mal, S. Nori, C. Jin, J. Narayan, S. Nellutla, A. I. Smirnov, and J. T. Prater, J. Appl. Phys. **108**, 073510 (2010); S. Mal, S. Nori, J. Narayan, J. T. Prater, and D. K. Avasthi, Acta Mater. **61**, 2763 (2013).
[35]S. Pal, A. Sarkar, S. Chattopadhyay, M. Chakrabarti, D. Sanyal, P. Kumar, D. Kanjilal, T. Rakshit, S. K. Ray, and D. Jana, Nucl. Instrum. Methods Phys. Res. B **311**, 20 (2013).
[36]B. D. Cullity, *Elements of X-Ray Diffraction* (Addison-Wesley Publishing Company, Philippines, 1978).
[37]M. A. Garcia, E. F. Pinel, J. de la Venta, A. Quesada, V. Bouzas, J. F. Fernández, J. J. Romero, M. S. M. González, and J. L. C. Krämer, J. Appl. Phys. **105**, 013925 (2009).
[38]P. Sharma, A. Gupta, F. J. Owens, A. Inoue, and K. V. Rao, J. Magn. Magn. Mater. **282**, 115 (2004); H. J. Blythe, R. M. Ibrahim, G. A. Gehring, J. R. Neal, and A. M. Fox, *ibid.* **283**, 117 (2004).
[39]S. Dutta, S. Chattopadhyay, D. Jana, A. Banerjee, S. Manik, S. K. Pradhan, M. Sutradhar, and A. Sarkar, J. Appl. Phys. **100**, 114328 (2006).
[40]S. Dutta, S. Chattopadhyay, A. Sarkar, M. Chakrabarti, D. Sanyal, and D. Jana, Prog. Mater. Sci. **54**, 89 (2009).
[41]A. P. Hynes, R. H. Doremus, and R. W. Siegel, J. Am. Ceram. Soc. **85**, 1979 (2002).
[42]E. Şenadim, H. Kavak, and R. Esen, J. Phys.: Condens. Matter **18**, 6391 (2006).
[43]S. Dutta, M. Chakrabarti, S. Chattopadhyay, D. Jana, D. Sanyal, and A. Sarkar, J. Appl. Phys. **98**, 053513 (2005).
[44]J. J. Richardson, G. K. L. Goh, H. Q. Le, L.-L. Liew, F. F. Lange, and S. P. DenBaars, Cryst. Growth Des. **11**, 3558 (2011).
[45]S. W. H. Ejit, A. van Veen, H. Schut, P. E. Mijnarends, A. B. Denison, B. Barbiellini, and A. Bansil, Nature Mater. **5**, 23 (2006).
[46]R. Vidya, P. Ravindran, E. Fjellvåg, B. G. Svensson, E. Monakhov, M. Ganchenkova, and R. M. Nieminen, Phys. Rev. B **83**, 045206 (2011).
[47]A. Chakrabarty and C. H. Patterson, Phys. Rev. B **84**, 054441 (2011).
[48]G. Brauer, W. Anwand, W. Skorupa, J. Kuriplach, O. Melikhova, C. Moisson, H. V. Wenckstern, H. Schmidt, M. Lorenz, and M. Grundmann, Phys. Rev. B **74**, 45208 (2006).
[49]S. Chattopadhyay, S. K. Neogi, P. Pandit, S. Dutta, T. Rakshit, D. Jana, S. Chattopadhyay, A. Sarkar, and S. K. Ray, J. Lumin. **132**, 6 (2012).
[50]A. Janotti and C. G. Van de Walle, Phys. Rev. B **76**, 165202 (2007).
[51]C. Drouilly, J.-M. Krafft, F. Averseng, S. Casale, D. B. Bachi, C. Chizallet, V. Lecocq, H. Vezin, H. L. Pernot, and G. Costentin, J. Phys. Chem. C **116**, 21297 (2012).
[52]B. Panigrahi, M. Aslam, D. S. Misra, M. Ghosh, and D. Bahadur, Adv. Funct. Mater. **20**, 1161 (2010).
[53]P. Zhan, W. Wang, C. Liu, Y. Hu, Z. Li, Z. Zhang, P. Zhang, B. Wang, and X. Cao, J. Appl. Phys. **111**, 033501 (2012).
[54]B. J. Jin, S. Im, and S. Y. Lee, Thin Solid Films **366**, 107 (2000).
[55]M. Ruth and C. Meier, Phys. Rev. B **86**, 224108 (2012).
[56]A. K. Mishra, S. K. Chaudhuri, S. Mukherjee, A. Priyam, A. Saha, and D. Das, J. Appl. Phys. **102**, 103514 (2007).
[57]I. Shalish, H. Temkin, and V. Narayanamurti, Phys. Rev. B **69**, 245401 (2004).
[58]C. T. That, L. Weston, and M. R. Phillips, Phys. Rev. B **86**, 115205 (2012).